Electronic Magnetic Gearing Motor Analyses and Simulations for Electric Vehicles

Xiao GUO [1], GuoPing Liu [1], Nabeel Shirazee [2], Jonathan Williams [1]

[1] Faculty of Advanced Technology, University of South Wales, Pontypridd CF37 1DL, UK
[2] Electronica Products Limited, Suffolk House, Trade Street, CARDIFF, CF10 5DT, UK

Abstract: This paper presents an innovative electronic-magnetic geared motor technology for electric vehicles. The motor has been designed and simulated. The electronic-magnetic gearing (EMG) connects parallel, series or hybrid connections of stator windings into gears to accommodate the different speed and torque demands in the drive cycle. The objective of the EMG is to increase the speed and torque range of the motor and reduce current draw from the batteries. A 1.5kW prototype EMG motor was built and tested on a test rig at Electronica Products Ltd. A comparison simulation of an EMG motor compared with a traditional permanent magnet synchronous motor (PMSM) was also carried out. The result proves that the theory of EMG is sound and it has great potential for energy efficiency in electric vehicles (EVs), especially for the powertrain units.

Keywords-components: Motor for hybrid electric vehicle, traction motor, energy saving motor, reduced current draw motor, high torque electric motor, motor for electric vehicle.

1. Introduction

Traditional ICE (Internal combustion Engine) vehicles rely on fossil fuels such as diesel and petrol. The automotive industry is one of the largest energy consumers of petroleum products. To cut down on emissions and reduce their dependency on fuels, vehicle manufacturers are developing new techniques while performing extensive research on EVs (Electric Vehicle). Governments around the world are also introducing policies to encourage people to buy low emission vehicles. In 2011, the UK government announced the “Plug-in car and van grants”. Since then more and more people in the UK have chosen to buy a zero-emission electric vehicle. [1] The electric car market in the UK reached a record high in the first three months of 2016. [2].

An EV is normally driven by electric motors, which are powered by ESUs (energy storage units), such as a battery, a supercapacitor or a hydrogen fuel cell. However, no matter what kind of ESU is chosen, it supplies the same electric power. Due to this limited on-board power source, EVs normally allow only a very short driving range compared with traditional ICE vehicles.

Nissan Leaf and BMW i3 are the top two bestselling EVs currently in the UK market. The latest version of the Nissan Leaf is powered by a 30kWh battery, which when fully charged can allow the car to drive 172km (107 miles) in a standard city traffic condition. The official range of a BMW i3e is 130 to 160 km (80 to 100 miles) for the 60Ah battery option under the New European Driving Cycle (NEDC). None of these top selling EVs give a driving range longer than 200km. The short driving range is the biggest issue for EVs. The solutions are either to increase the battery pack size or to improve the system’s energy consumption efficiency, especially the efficiency of the electric motor.

Many different kinds of motors have been tested on EVs, the most commonly used one is the permanent magnetic (PM) brushless DC motor. It has the advantages of higher efficiency and a lower susceptibility to mechanical wear. With the modern control methods such as vector control or direct torque control, a DC motor gives a much better dynamic performance when used on EVs.

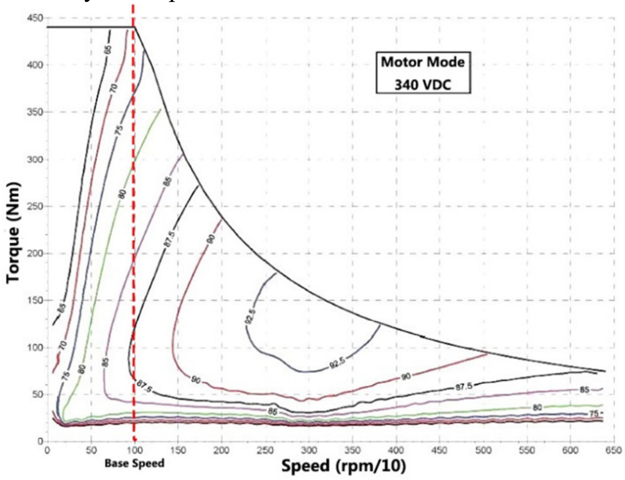

Fig. 1. *Speed-torque curve of a PM brushless DC motor, Motor A.*

Fig.1 shows a real speed-torque curve from a permanent magnetic brushless DC motor. This motor A is designed for electric and hybrid vehicles and is now selling in the US market. In this curve, the motor has a constant torque below the base speed and a constant power beyond the base speed. In this way, there comes a trade-off problem between starting torque and constant power range. From a vehicle dynamics point of view, when the vehicle starts up, accelerates or climbs up a hill, the output torque from the motor should be as high as possible to enhance the cars performance.

Researchers are starting to think about new ways to design motors to overcome this speed-torque problem. Huang and Chang [3] proposed an electrical two-speed propulsion system by switching induction motor windings between a serial connection for starting an electric vehicle and a parallel connection for normal speed operation. Yang and Wang [4] made use of a winding changeable axial flux DC motor with a group of supercapacitors. The supercapacitors are connected in serial or parallel with the motor at different gears. This system required many IGBT switches and diodes, which made it very bulky and expensive. Moreover, the axial flux design is not suitable for high dynamic performance use in EVs. For these previous researches, the motor efficiency issue is not considered at gear switching.

This paper presents an innovative design of radial flux permanent magnetic brushless DC motor with Electronic Magnetic Gearing (EMG), in which the configuration of the windings is changed while the motor is operating. This method improves the starting torque performance and also increases the range of constant power by altering the winding configuration, “gear shifting”. The EMG system has been patented by Electronica Products Limited.

2. Design of electronic magnetic gearing

A normal 3-phase radial flux brushless DC motor can be simplified as in Fig 2. The stator has windings all around it and the rotor rotates in the center. The rotor is made with permanent magnets.

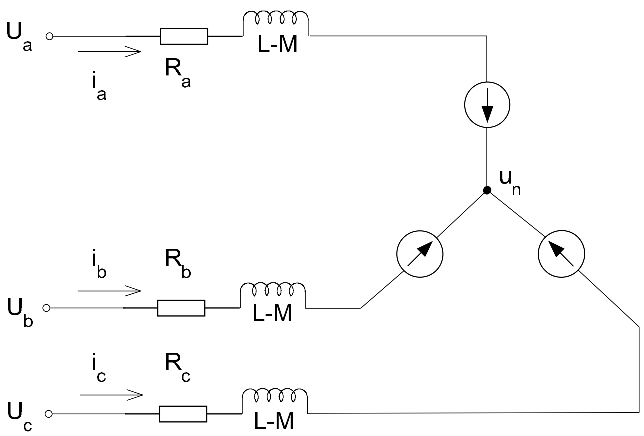

Fig. 2. *Electric circuit of a brushless DC motor*

A normal 3-phase radial flux brushless DC motor can be simplified expressed as the following equation:

$$\begin{bmatrix} u_a \\ u_b \\ u_c \end{bmatrix} = \begin{bmatrix} R_s & 0 & 0 \\ 0 & R_s & 0 \\ 0 & 0 & R_s \end{bmatrix} \begin{bmatrix} i_a \\ i_b \\ i_c \end{bmatrix} + p \begin{bmatrix} L_a & M_{ab} & M_{ac} \\ M_{ba} & L_b & M_{bc} \\ M_{ca} & M_{cb} & L_c \end{bmatrix} \begin{bmatrix} i_a \\ i_b \\ i_c \end{bmatrix} + p \begin{bmatrix} \psi_r^a \\ \psi_r^b \\ \psi_r^c \end{bmatrix} \quad (1)$$

Where u_A, u_B and u_C are the voltages of the 3-phase windings in each phase; i_a, i_b and i_c are currents of the 3-phase windings in each phase; ψ_r^a , ψ_r^b and ψ_r^c are the permeant magnetic flux linkage projection components on each winding; p is the differential operator; L_a, L_b and L_c are the inductances on each of the windings; M_{ab}, M_{ac}, M_{ba}, M_{bc}, M_{ca} and M_{cb} are the mutual inductances between the three windings.

After Clarke transform and Park transform, the PMBLDC’s voltages in the d-q system can be expressed as follows:

$$\begin{bmatrix} u_d \\ u_q \end{bmatrix} = R_s \begin{bmatrix} i_d \\ i_q \end{bmatrix} + \begin{bmatrix} L_d & 0 \\ 0 & L_q \end{bmatrix} p \begin{bmatrix} i_d \\ i_q \end{bmatrix} + \omega \begin{bmatrix} 0 & -L_q \\ L_d & 0 \end{bmatrix} \begin{bmatrix} i_d \\ i_q \end{bmatrix} + \omega \begin{bmatrix} \psi_f \\ 0 \end{bmatrix} \quad (2)$$

The flux linkage in d-q system is:

$$\begin{bmatrix} \psi_d \\ \psi_q \end{bmatrix} = \begin{bmatrix} L_d & 0 \\ 0 & L_q \end{bmatrix} \begin{bmatrix} i_d \\ i_q \end{bmatrix} + \begin{bmatrix} \psi_f \\ 0 \end{bmatrix} \quad (3)$$

And the torque in d-q system is:

$$T_{em} = \psi_s i_s = p_n\left[\psi_f i_q + \left(L_d - L_q\right) i_d i_q\right] \quad (4)$$

Where p_n is the number of pole pairs, ψ_f is the permanent magnetic flux linkage, L_d and L_q are the inductances on the d-q axis and i_d and i_q are the currents on the d-q system.

Definition: The stator current’s space vector is i_s. It is in the same phase as stator’s flux linkage vector ψ_s. The angle between stator’s flux linkage and the permanent magnetic flux linkage is β, so the current in d-q system is:

$$\begin{cases} i_d = i_s cos\beta \\ i_q = i_s sin\beta \end{cases} \quad (5)$$

Take equation (5) into equation (4):

$$T_{em} = p_n\left[\psi_d i_q - \psi_q i_d\right] = p_n \psi_f i_s sin\beta + \frac{1}{2} p_n \left(L_d - L_q\right) i_s^2 sin2\beta \quad (6)$$

Equation (6) shows the PMSM’s torque in 2 parts. One is the electromagnetic torque generated by the magnetic field and the other one is the resistance torque generated by the salience effect.

In the steady state of a PMSM, ignoring the effect from the resistance, from equation (2) and (3) we can get the motor speed [5]

$$\begin{cases} u_d = -\omega L_q i_q \\ u_q = \omega L_d i_d + \omega \psi_f \end{cases} \quad (7)$$

So the speed of motor can be expressed as:

$$\omega = \frac{u}{\sqrt{(L_q i_q)^2 + (L_d i_d + \psi_f)^2}} \quad (8)$$

$$\omega = \frac{u_{max}}{\sqrt{\left(L_q i_q\right)^2 + \left(L_d i_d + \psi_f\right)^2}} = \frac{u_{max}}{\sqrt{(L_q i_s cos\beta)^2 + (\psi_f - L_d i_s sin\beta)^2}} \quad (9)$$

where u_{max} is the maximum voltage of the inverter.

Definition: ξ is the demagnetizing coefficient, the ratio of the d-axis armature reaction flux to the permanent magnet flux-linkage [6]

$$\xi = \frac{L_d i_s}{\psi_f} \quad (10)$$

Definition: Saliency coefficient ρ is the ratio of L_d and L_q [7]

$$\rho = \frac{L_d}{L_q} \quad (11)$$

Take (10) and (11) into equation (9), then the base speed of a PMSM is:

$$\omega = \frac{u_{max}}{\psi_f\sqrt{(\rho\xi cos\beta)^2 + (1-\xi sin\beta)^2}} \quad (12)$$

Phase A of a motor's stator will be analyzed as a sample phase. If all windings of phase A are simplified into 2 turns, and these 2 turns of windings connect all IGBT switches in the following way, it will make a simple circuit shows in Fig 3.

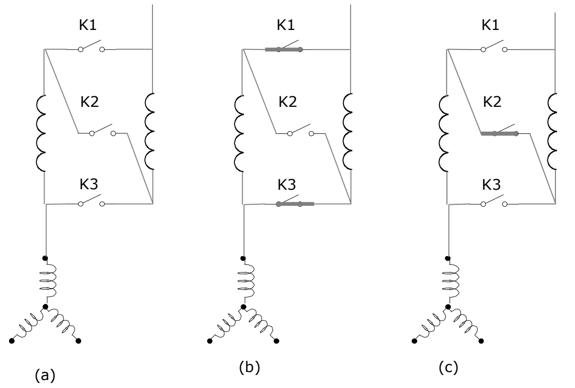

Fig. 3. *Various On/Off settings of switches in one phase of an EMG motor system.*

In Fig 3(a), all switches are open (Off). There is no current passing through and no torque generated. In Fig 3(b), switches K1 and K3 are closed (On) and K2 is open (Off); the windings are connected in parallel. In Fig 3(c) switch K2 is On and switches K1 and K3 are Off; the windings are connected in series. If the windings change from full series to full parallel, the changes of inductance and flux linkage will be as follows.

$$L_d^s = 4L_d^p;\ L_q^s = 4L_q^p;\ \psi_f^s = 2\psi_f^p \quad (13)$$

Take (13) into equation (6) and (12),

$$T_{em}^s = 2T_{em}^p + \left(L_d^p - L_q^p\right)i_{max}^2 sin2(\beta^p + 90) \quad (14)$$

and

$$\frac{\omega_{max}^s}{\omega_{max}^p} = \frac{\sqrt{[\rho\xi^p\sin(\beta^p+90)]^2 + [1+\xi^p\cos(\beta^p+90)]^2}}{2\sqrt{[2\rho\xi^p\sin(\beta^p+90)]^2 + [1+2\xi^p\cos(\beta^p+90)]^2}} \quad (15)$$

In an EMG motor, the saliency coefficient ρ is 1, where Ld=Lq and β =0, so that the equations can be simplified to

$$T_{em}^s = 2T_{em}^P \quad (16)$$

$$\frac{\omega_{max}^s}{\omega_{max}^p} = \frac{\sqrt{1+(\xi^p)^2}}{2\sqrt{1+4(\xi^p)^2}} \quad (17)$$

From the above equations we can see, after windings change from series to parallel, the maximum torque output is reduced to half and the base speed is increased.

3. EMG motor test rig and configuration

Following the variable winding change theory, a prototype Electronic Magnetic Gearing (EMG) motor and a system test rig was built up for a 1.5 kW EMG motor. The motor was driven by a full bridge driver which was connected to a lithium-ion battery. The speed and torque demands could be read either from a drive cycle profile or adjusted manually. The IGBT switches On/Off signals were generated from the controller and sent to the switches, these signals followed a pre-setup rule for different motor gear shifts.

The test rig setup of the 1.5 kW prototype EMG motor is shown in Fig 4. In the practical test, a PMBLDC motor was used as a load to simulate the different resistances of a road.

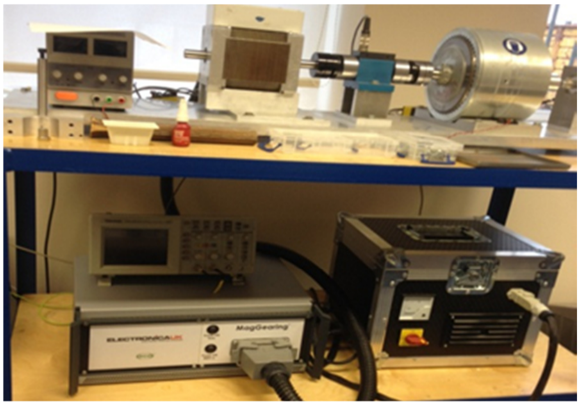

Fig. 4. *Test rig setup of the 1.5kW EMG motor.*

Fig. 5 shows the speed-torque test results from the 1.5kW EMG motor with three gears. Profile 1 is series (gear 1), profile 2 is series/parallel (gear 2) and profile 3 is parallel (gear 3) connection. These profiles were mapped in the electronic drive which gave the most suitable drive option depending on the speed-torque requirement and the optimum motor efficiency. The gears could shift manually or automatically at the switching points.

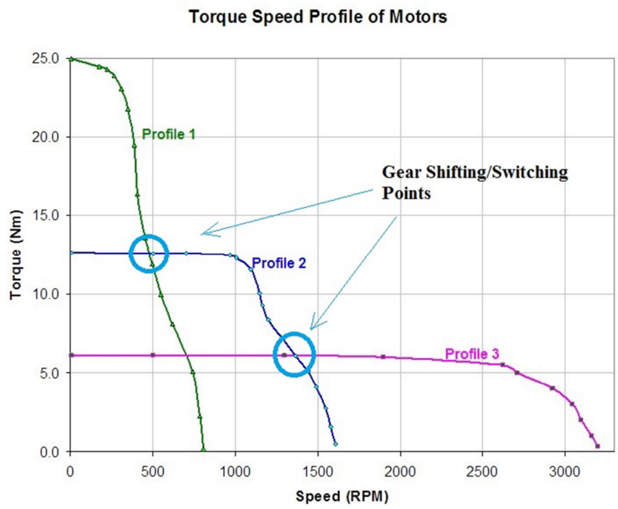

Fig. 5. *Test result of 3 gears in 1.5kW EMG motor.*

The test results showed that the base speed nearly doubled with every up-shift of the gear from 1 to 3. The torque nearly doubled with every down-shift of the gears from 3 to 1. These results were used to examine equations (16)-(19) to see whether they were correctly applied.

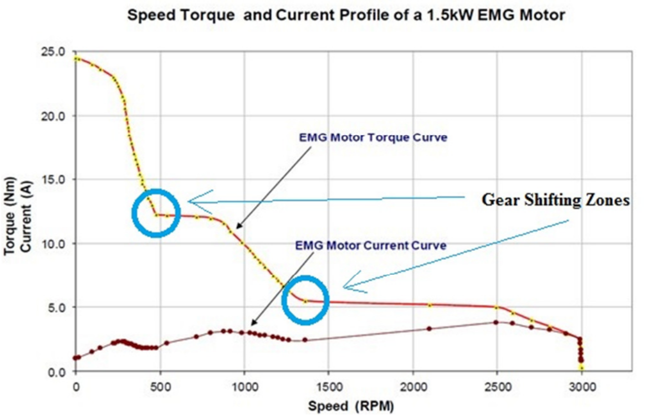

Fig. 6. *Speed-torque and current curve of 1.5kW EMG motor.*

In practice, the 1.5 kW EMG motor operated with a speed-torque curve shown in Fig. 6. The rated torque and change in the base speed of the gears is also shown. The test results showed that the current stays low and almost at the same level in all gears. Therefore, by using the EMG motor for different speed and torque demands, one can always get better energy efficiency out of the batteries. Compared with the traditional PMSM, the EMG motor also covers a much larger working speed range without using high field weakening and the inefficiencies associated with it.

4. 50kW EMG motor model simulation

Motor A, shown in Fig. 1, is a 50kW PMSM motor designed for EVs and hybrid vehicles. To compare the performance of an EMG motor with this traditional PMSM, another 50kW EMG motor was designed using MotorSolve / Infolytica software. MotorSolve is a static simulation software that cannot simulate a dynamic winding changing process, however the motor parameters are shown in Fig. 7.

Rated Voltage	400	Volts
Rated Current	125	Amps
Peak Amps	163	Amps
Length	240	mm
Diameter	180	mm
Weight	38	kg
Absolute Peak Power	65	kW
Nominal Power	50	kW
Peak Torque (Gear 1)	2350	Nm
Peak Torque Density	61.8	Nm/kg
Peak Power Density	1.7	kW/kg
Maximum efficiency	95%+	

Fig. 7. Specifications of the 50kW EMG motor simulated using MotorSolve.

All four gears were simulated separately with different winding settings. Winding setting is changed by changing the "number of stands in hand" and the "number of turns". In the simulation, the setting of different gears is shown in the table 1.

Table 1. Gears setting in MotorSolve for EMG motor.

Gears	Number of stands in	Number of turns
Gear 1	1	24
Gear 2	2	12
Gear 3	4	6
Gear 4	8	3

Following equation (16), the base torques in these 4 gears should have the following relationship.

$$T_{em}^{gear1} = 2T_{em}^{gears2} = 4T_{em}^{gear3} = 8T_{em}^{gear4} \quad (18)$$

The simulation results of the four gears are shown in Fig. 8 below.

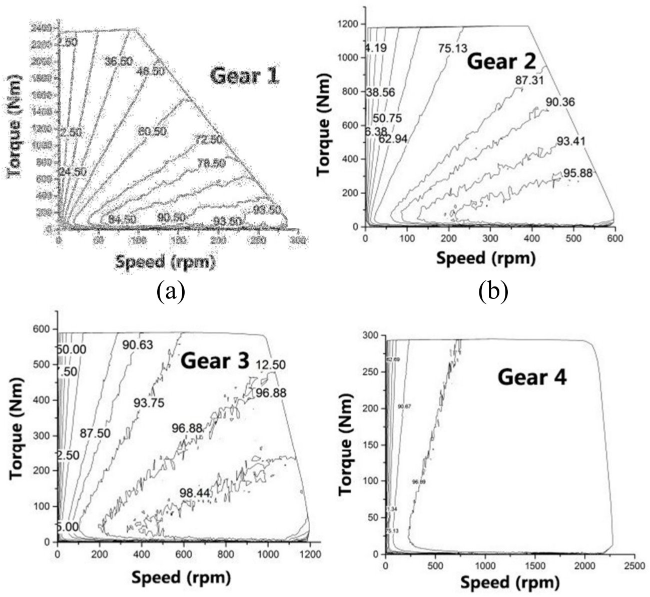

(a) (b) (c) (d)

Fig. 8. *Speed-Torque curves for four gears in a 50kW EMG motor.*

Previous researches have not considered the dynamic efficiency of a motor in different gears. Different gears in the motor have different efficiency map curves. In this research, ISO efficiency curves for all the gears are plotted and analyzed. The speed-torque curves in Fig.8 show the various efficiency plot lines with different working points of an EMG motor.

The simulation results prove equation (18) to be correct and the rated torque of each gear is double that of the gear below. Fig. 9 shows results for all the gears in one figure to give a clearer view of the simulation results. Compared with a traditional motor, the EMG technology increases the working range of speed and torque of an electric machine. If an electric vehicle is driven by an EMG motor, it will accelerate faster with a larger starting torque and it will also have a much higher maximum cruising speed.

In Fig 9, some speed-torque demand areas are covered by more than one gear. This means that more than one winding setting can meet that speed and torque demand. In practical use, the controller for the EMG gear selection will check the pre-load efficiency curves for different gears, and choose the gear with the highest efficiency at that speed and torque demand point. This EMG technology will give an electric machine a better performance based on energy efficiency.

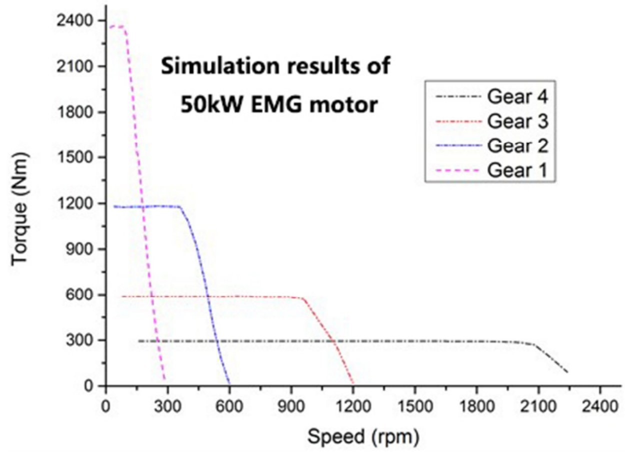

Fig. 9. *EMG motor's speed torque curve of gear 1-4.*

5. Simulation of EMG motor in an EV

Simulation results show that an EMG system has huge potential benefits to EVs with energy saving. The 50kW Motor A and 50kW EMG motor will be simulated in AVL/Cruise* under the EV model.

In a traditional EV set up with the motor connected using a fixed ratio final drive. The vehicle specification is used from an EV related project conducted by a UK company.

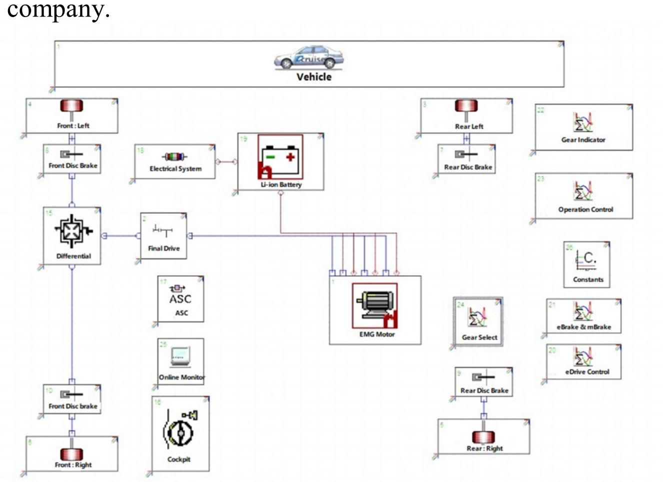

Fig. 10. *Electric Vehicle Model with Motor A.*

The EV model with EMG motor is shown in Fig. 10. The vehicle specification is the same as the one with Motor A. An EMG model block was built, with 4 different motors combined together. Each motor has the profile of one gear in the 50kW EMG motor range. The load signal of each motor is controlled by a gear selection block.

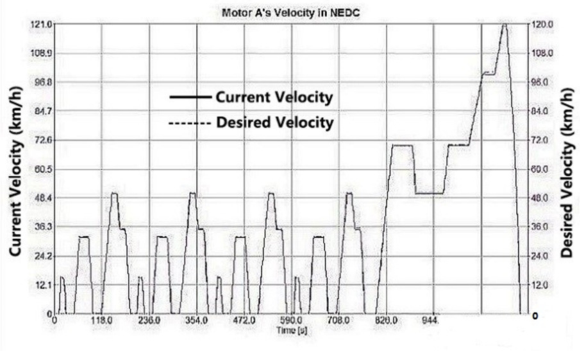

(a)

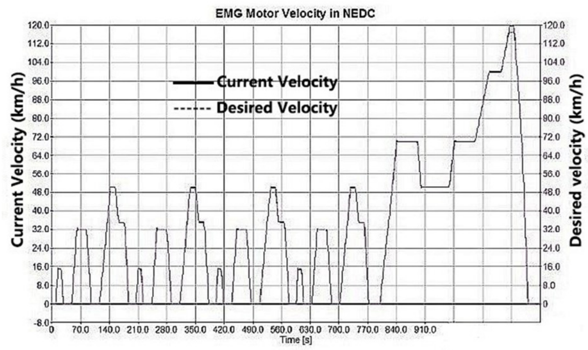

(b)

Fig. 11. *Simulation results from Motor A and EMG motor for a NEDC.*

The simulation results from Motor A and EMG motor are shown in Fig. 11.

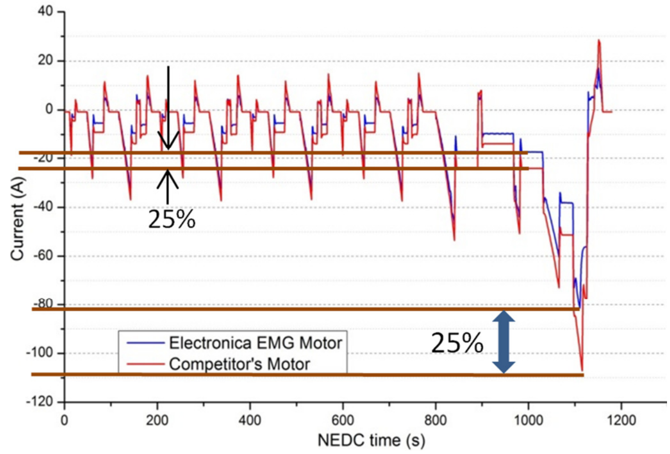

Fig. 12. *Currents of Motor A and EMG motor in NEDC.*

The current difference between Motor A and the EMG motor is shown in Fig. 12. On average, for the EMG motor, the overall drive cycle current is about 25% less than that of the Motor A's current. This means that the EMG motor uses less energy than motor A for the same drive cycle. Also, lesser currents will increase the driving range of the EV and will extend the usage life of the battery pack.

The State of Charge (SOC) of Motor A and EMG motor is shown in Fig. 13. In the EV driving with Motor A, the starting SOC is 95% and at the end the SOC is around 85%. This means that a complete NEDC cycle uses about 10% of total energy in the battery. In the EV driven by EMG motor, the starting SOC is 95% and at the end of the drive cycle the SOC is around 87%. This means that a complete NEDC cycle uses about 8% of the total energy from the battery. The SOC result also proves that the EMG motor uses less electricity in the same drive cycle.

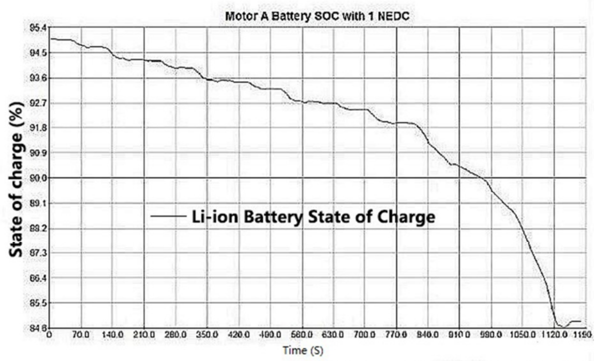

(a)

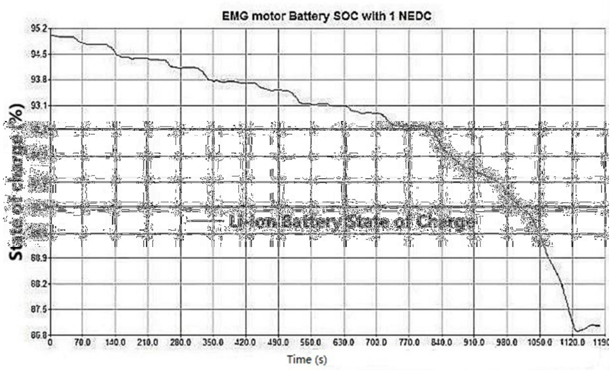

(b)

Fig. 13. *SOC of Battery with Motor A and EMG motor in NEDC.*

Fig.14 shows the driving range test results for Motor A and the EMG motor. The drive cycle profile is ten NEDCs in total. The EV with Motor A drives a range of 98,000m and an EV with the EMG motor drives 110,000m. In this test, an EV with an EMG motor has a drive range of about 12.2% longer than the EV with Motor A. Motor A used up all the energy on board and the EV with the EMG motor still had 3% energy left over in the batteries.

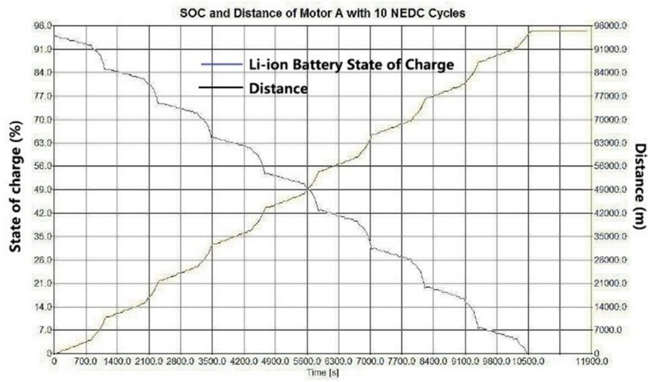

(a)

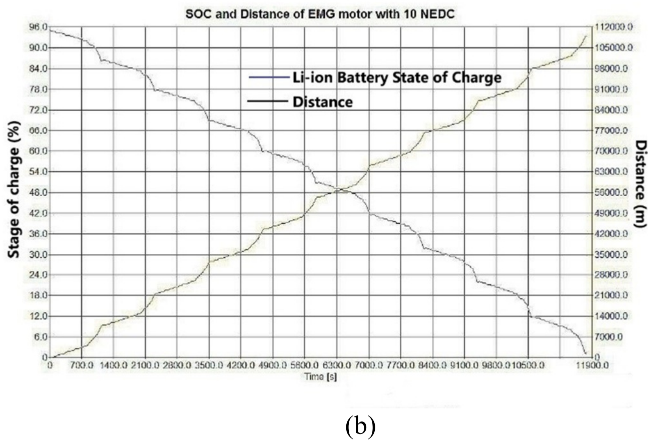

(b)

Fig.14. *SOC of Battery and driving range of EVs with Motor A and EMG motor in 10 NEDC.*

6. Summary and conclusions

In this research, an innovative radial flux EMG motor has been successfully analyzed, simulated, built and tested on a test rig. The electronic controller was designed and built for an automatic gear selection by the speed/torque demand and the gear efficiency algorithms. In the experimental tests, when the gears changed at the shift points, the system had a slight step movement. Therefore, field weakening applied at the gear shifting zones would make the system speed-torque curve smooth and eliminate the step movement.

A 50kW EMG motor model was designed using MotorSolve/Infolytica software. This 50kW EMG motor was compared with a 50kW motor A already selling in the US market for hybrid/electric vehicles. The EMG motor showed to increase the starting torque and extend the operational speed range of the vehicle compared with traditional motors. The simulation results proved that the EMG motor technology improves the efficiency of the whole EV system by a wide margin and it is a technology that could be soon adopted by the industry.

For a complete NEDC cycle the EMG motor needed 25% less average current to operate than motor A. Further, over ten NEDCs, the EMG motor increased the driving range by about 12.2% with 3% still leftover in the batteries. The EMG motor showed to work extremely well and it has great potential for saving energy, increasing battery life and therefore increasing the overall performance of the powertrain used in electric vehicles. All simulations ignored the energy consumption by the IGBT switches and the ancillary electronic hardware. Hence, the true energy savings will be slightly lower than the simulation results.

References

[1] 'Plug-in car and van grants', https://www.gov.uk/plug-in-car-van-grants, accessed 27 January 2017

[2] 'Goultralow.com report', https://www.goultralow.com/press-centre/releases/electric-car-registrations-reach-record-high-plug-popularity-continues-grow/, accessed 27 January 2017

[3] Huang, H., Chang, L.: 'Tests of electrical-two-speed propulsion by induction motor winding switching for electric vehicles', IEEE 47th Vehicular Technology Conference., 1997, (3), pp 1907-1911

[4] Yang, Y., Liu, J.: 'An Electric Gearshift With Ultracapacitors for the Power Train of an Electric Vehicle With a Directly Driven Wheel, IEEE Transactions on Motor Vehicular Technology 2007, Volume: 56, (5), pp 2421-2431

[5] Morimoto, S., Sanada, M.: 'Inverter-driven synchronous motors for constant power'. IEEE Industry Applications Magazine, 1996, 2, (6)

[6] Morimoto, S., Takeda, Y.: 'Expansion of operating limits for permanent magnet motor by optimum flux-weakening' Conference Record of the IEEE Industry Applications Society Annual Meeting, 1989, (1), pp: 51 - 56

[7] Morimoto, S., Takeda, Y.: 'Expansion of Operating Limits for Permanent Magnet Motor by Current Vector Control Considering Inverter Capacity', IEEE Transactions on Industry Applications, Sep/Oct 1990, 26, (5)